

Empirical correlations of drug-and plant-based bioactive compound solubility in supercritical CO₂: A comparative evaluation study

Christine Ann Obek^a, Agus Saptoro^{a,b,*}, Angnes Ngieng Tze Tiong^a, Zeinab Abbas Jawad^c, Zong Yang Kong^d, Suryadi Ismadji^e, Jaka Sunarso^f

^a Department of Chemical and Energy Engineering, Curtin University Malaysia, CDT 250, Miri, 98009, Sarawak, Malaysia

^b Curtin Malaysia Research Institute (CMRI), CDT 250, Miri, 98009, Sarawak, Malaysia

^c Department of Chemical Engineering, College of Engineering, Qatar University, P.O. Box: 2713, Doha, Qatar

^d Department of Engineering, School of Engineering and Technology, Sunway University, Bandar Sunway 47500, Selangor, Malaysia

^e Department of Chemical Engineering, Widya Mandala Surabaya Catholic University, Kalijudan 37, Surabaya 60114, Indonesia

^f Research Centre for Sustainable Technologies, Faculty of Engineering, Computing and Science, Swinburne University of Technology, Kuching 93350, Malaysia

ARTICLE INFO

Keywords:

Solubility
Bioactive compounds
Density-based model
Molecular structure
Supercritical carbon dioxide

ABSTRACT

Over the last few decades, supercritical fluid extraction process has greatly assisted the search for more medicinal and therapeutic properties of bioactive compounds from an extensive range of botanical matrices. The yield of supercritical fluid extraction is often limited by the solubility of a targeted solute in the solvent and thus knowledge on solubility has become one of the fundamental variables of interest in the extraction process. However, the studies to evaluate the performance of density-based empirical models in estimating the solubility of different drug- and plant-based bioactive compounds were scarce. Therefore, this study aimed to gather the solubility data of 33 drugs and 40 plant-based bioactive compounds at varying temperatures and pressures and correlated them with 26 most widely used density-based models. The solubility data were critically analysed and reported from two perspectives: well-studied solubility-influencing factors such as pressure, temperature, and additional influencing factors what o such as molecular structure and weight. Then, a thorough evaluation of the existing empirical solubility models involving 26 predictive models for 73 bioactive compounds was performed. From the results and findings, it was evident that the 8-parameter Belghait et al. model showed the overall highest accuracies indicated by the lowest absolute average relative deviation of 7.42 %, 10.16 %, and 6.57 %, respectively for all bioactive compounds, drug-based bioactive compounds, and plant-based bioactive compounds. Belghait et al. model is also superior since its predictive performances are the best for 54 % of the bioactive compounds studied. Meanwhile, Kumar and Johnston's, Sung and Shim's, and Sodeifian et al's models demonstrated the best solubility predictions for 3-, 4-, and 6-parameter empirical models, respectively, for both plant and drug-based compounds. As the effects of pressure and temperature on solubility have widely acknowledged, this study also highlights the influence of molecular structure complexity on solubility. The main findings from this comparative evaluation proved that density-based models are efficacious in predicting solubility of both plant and drug-based bioactive compounds.

1. Introduction

Conventional extraction techniques such as hydrodistillation, steam distillation, and Soxhlet extraction can be engaged to obtain targeted compounds from the plant materials albeit the associated disadvantages [32]. In finding a greener alternative to the conventional processes, research and development work related to the Supercritical Fluid Extraction (SFE) technology is gaining recognition by industrial players

[33]. Unlike conventional extraction processes, SFE processes require a supercritical solvent obtained by heating and pressurizing the fluid beyond its critical point. Fluids at supercritical conditions typically exhibit properties of both liquid and gas, has density capable of dissolving a solute, and possess a low viscosity to facilitate more rapid mass transfer. The low operating temperature used in the supercritical fluid technologies (SFT) is the major advantage and the underlying reason that prevents thermal decomposition of heat-sensitive compounds

* Corresponding author.

E-mail address: agus.saptoro@curtin.edu.my (A. Saptoro).

<https://doi.org/10.1016/j.fluid.2024.114061>

Received 13 December 2023; Received in revised form 1 February 2024; Accepted 17 February 2024

Available online 18 February 2024

0378-3812/© 2024 The Authors. Published by Elsevier B.V. This is an open access article under the CC BY-NC-ND license (<http://creativecommons.org/licenses/by-nc-nd/4.0/>).

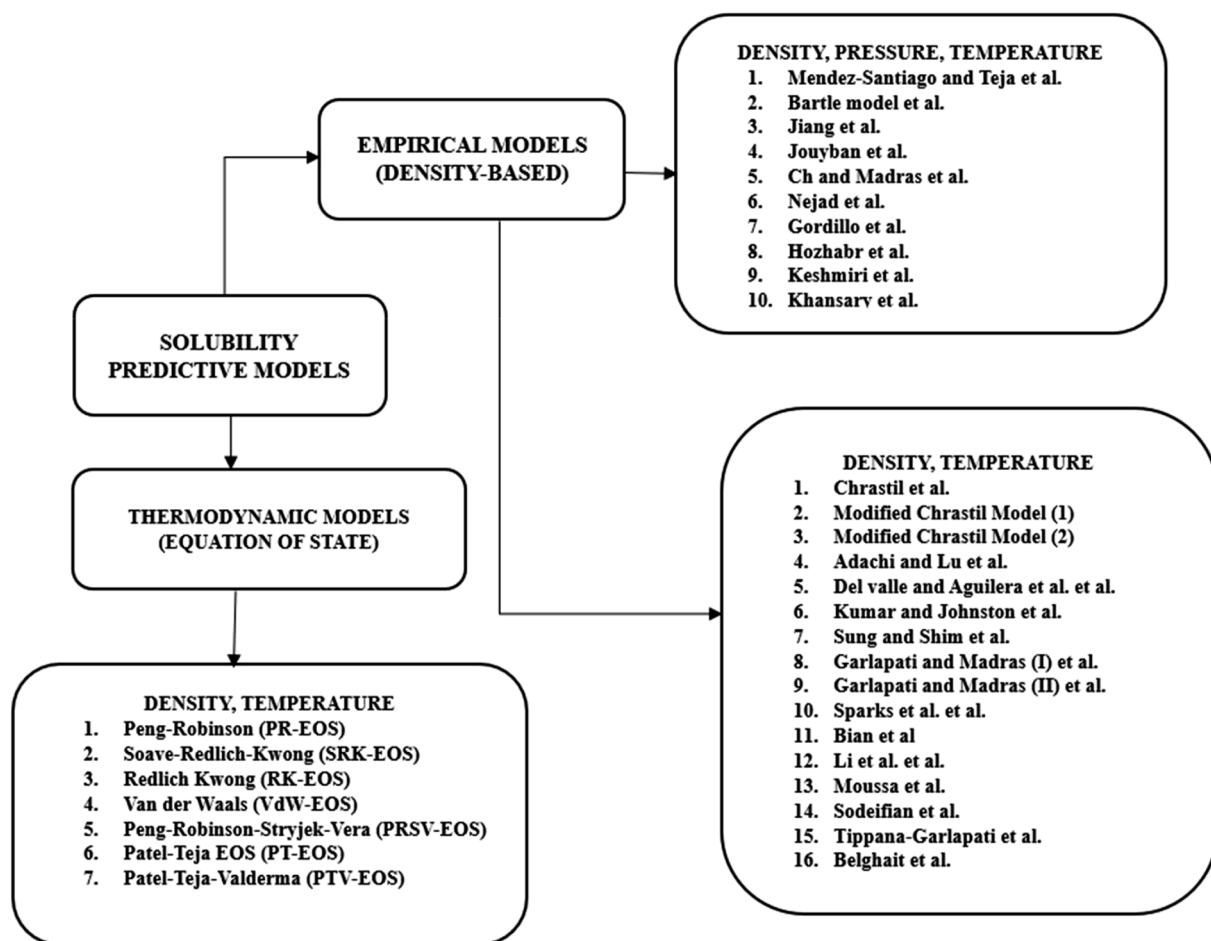


Fig. 1. An overview on the solubility modeling tools.

extracted if compared to the classical extraction methods [51,62]. The wide usage of supercritical carbon dioxide (SC-CO₂) in SFT is owing to its various features such as environmentally-friendly, generally recognized as safe solvent, its moderate critical temperature and pressure (304 K and 73.7 bar, respectively), offers high selectivity, and is easily attainable [3,95].

It is imperative to understand the solubility behavior of a solute in supercritical systems in order to scale up the SFE facilities, evaluate the process effectiveness, and carry out the process optimization and feasibility studies [10,59,108]. This is simply due to the fact that the extraction rate and yield of a solute is limited by its solubility in any given supercritical fluid [107]. In other words, a solute that possesses a good solubility in supercritical fluid expedites extraction and therefore reduces the experimental time [10]. A large majority of the published literatures focus on extraction studies, while less are targeted towards solubility studies and their modeling due to their greater complexity. Although solute solubility data can be experimentally measured at different temperatures and pressures, it is often difficult, expensive and time consuming [52]. As such, modeling tools in the form of empirical equation (density-based models) and thermodynamic equation of state (EOS) have been developed to correlate and predict solubility data especially at higher pressures and temperatures. This study aims to comprehensively report and critically evaluate 26 existing empirical models using the solubility data of 33 drugs and 40 plant-derived bioactive compounds.

2. Classification of solubility-predictive models

An overview of some commonly adopted solubility-predictive models is shown in Fig. 1. From Fig. 1, the solubility models are typically categorized into empirical, and thermodynamic models, both of which are computed numerically. Nevertheless, the empirical equations are often the preferred choices due to their simplicity, accuracy, and their applicability to various types of compounds [52,80]; with the Chrastil Model being one of the pioneer models developed [95]. The simplicity of empirical models is owed to the use of only three solvent-independent variables (pressure, temperature, and density) in computing the solubility and the associated equation coefficients are easily attained by carrying out multiple regression of available data [95]. To date, the empirical equation with the most number of parameters is an 8-parameter model developed by Belghait et al. [12]. Literature review proves that many models are proposed over the years by modifying the existing models to strive for higher accuracy in predicted data.

Conversely, although the thermodynamic EOSs coupled with various mixing rules are also widely utilized, they are often less favorable due to the high equation complexity and the need for numerous critical and physicochemical data. These data such as fugacity, molar, volume, sublimation pressure, critical temperature and pressure, acentric factor, and vapor pressure are often less readily available [60]. The recent example of the use of thermodynamic EOSs coupled with various mixing rules can be found from the work of Abadian et al. [1]. As most critical and physicochemical data are temperature dependent and cannot be

Table 1
Equations of density-based models used in this study.

Empirical Model	Equation	
Chrastil Equation [16]	$\ln S = k \ln \rho_1 + \frac{a}{T} + b$	(1)
Adachi and Lu [2]	$\ln S = k \ln \rho + \frac{a}{T} + b$, where $k = (e_0 + e_1 \rho + e_2 \rho^2)$	(16)
Del Valle and Aguilera [22]	$\ln S = k \ln \rho_1 + \frac{a}{T} + \frac{b}{T^2} + c$	(7)
Mendez-Santiago and Teja [73]	$T \ln(y_2 P) = a + b \rho_1 + c T$	(2)
Bartle et al. [11]	$\ln\left(\frac{P}{P_{ref}}\right) = k(\rho - \rho_{ref}) + \frac{a}{T} + b$	(3)
Kumar and Johnston [46]	$\ln S = a + \frac{b}{T} + c \rho$	(5)
Jiang et al. [8]	$\ln S = a \rho + \frac{b}{T} + c \ln P + d$	(8)
Sung and Shim et al. [73]	$\ln S = \left(a + \frac{b}{T}\right) \ln \rho + \frac{c}{T} + d$	(9)
Gordillo et al. [29]	$\ln(y_2) = a + b P + c P^2 + d P T + e T + f T^2$	(20)
Jouyban et al. [42]	$\ln(y_2) = a + b P + c P^2 + d P T + e \frac{T}{P} + f \ln \rho$	(22)
Garlapati and Madras [27]	$\ln(y_2) = k \ln \rho_1 T + \frac{a}{T} + b$	(4)
Garlapati and Madras (II) [28]	$\ln(y_2) = a + b \ln \rho + c \rho \ln \rho + \frac{d}{T} + e \ln \rho T$	(14)
Sparks et al. [96]	$\ln(y_2) = (e_0 + e_1 \rho + e_2 \rho^2) \ln \rho_1 + \frac{a}{T} + \frac{b}{T^2} + c$	(23)
Ch and Madras [73]	$\ln(y_2) = (d - 1) \ln \frac{P}{P_s} + \frac{a}{T} + b \rho_1 + c$	(10)
Bian et al. [13]	$\ln(y_2) = (e_0 + e_1 \rho) \ln \rho_1 + \frac{a \rho}{T} + \frac{b}{T} + c$	(15)
Modified Chrastil Model (I) [97]	$\ln(y_2) = a \ln \rho + b \rho \ln \rho + \frac{c}{T} + \frac{d}{T} \rho + e$ (15a)	
Li et al. [73]	$\ln(y_2) = k \ln(\rho_1 T) + a \rho_1 + \frac{b}{T} + c$	(11)
Nejad et al. [60]	$\ln(y_2) = a + b P^2 + c T^2 + d \ln \rho$	(12)
Hozhabr et al. [35]	$\ln(y_2) = a + \frac{b}{T} + \frac{c \rho}{T} - d \ln P$	(13)
Keshmiri et al. ([13,44])	$\ln(y_2) = a + \frac{b}{T} + c P^2 + \left(d + \frac{e}{T}\right) \ln \rho_1$	(17)
Khansary et al. [9]	$\ln(y_2) = \frac{a}{T} + b P + c \frac{P^2}{T} + d \ln \rho_1 + e P \ln \rho_1$	(18)
Modified Chrastil Model (2) [7]	$\ln(y_2) = a \ln \rho + \frac{b}{\rho} \ln \rho + c \frac{\rho}{T} + d$ (6)	
Moussa et al. [77]	$\ln(y_2) = a + b \rho + c \rho^2 + d \rho T + e \frac{T}{\rho} + f \ln \rho$	(24)
Belghait et al. [12]	$\ln(y_2) = a + b \rho + c \rho^2 + d \rho T + e T + f T^2 + g \ln \rho + h/T$	(25)
Sodeifian et al. [87]	$\ln(y_2) = a + \frac{b P^2}{T} + c \ln \rho T + d(\rho \ln \rho) + e P \ln T + f \frac{\ln \rho}{T}$	(19)
Tippana-Garlapati [83]	$y_2 = (a + b P_r + c P_r^2) T_r^2 + (d + e P_r + f P_r^2)$	(21)

determined experimentally, appropriate equations and group contribution methods are to be carefully selected to compute these data [12,74]. Group contribution methods include the Ambrose Walton method for calculation of the sublimation pressure [82], Stein-Brown method to calculate the critical temperature [87], as well as Marrero and Ghani method to estimate the critical pressure [85]. Some of the commonly used EOSs are Peng-Robinson (PR-EOS) and Soave-Redlich-Kwong (SRK-EOS) coupled with Van der Waals mixing rules [93].

Although both categories of solubility models are commonly utilized, the main focus of this study is directed towards the performance of empirical models in correlating the solubility data of both plant and drug-based compounds. To the best of our knowledge, limited studies

Table 2
Density-based empirical models categorized according to the number of parameters

No. of parameters	Density-based model	No. of parameters	Density-based model
3	Chrastil Model	5	Adachi and Lu (AL)
3	Mendez-Santiago & Teja (MST)	5	Garlapati & Madras II
3	Bartle Equation	5	Bian et al.
3	Kumar and Johnston (KJ)	5	Keshmiri et al.
3	Garlapati & Madras (I)	5	Khansary et al.
4	Del Valle and Aguilera (DVA)	6	Modified Chrastil (1)
4	Modified Chrastil (2)	6	Gordillo et al.
4	Jiang et al.	6	Jouyban et al.
4	Sung and Shim (SS)	6	Sparks et al.
4	Ch and Madras (Ch-M)	6	Sodeifian et al.
4	Li et al.	6	Tippana-Garlapati
4	Nejad et al.	6	Moussa et al.
4	Hozhabr et al.	8	Belghait et al.

have been performed to evaluate the performance of density-based models on different categories of compounds. One of the few excellent reviews was carried out by Antonie and Pereira [8] in correlating the solubility data using four density-based models. Nonetheless, a comprehensive review on the performance of 26 existing models in correlating data of both plant and drug-based bioactive compound has not been performed. Hence, the objective of this study is to compile the solubility data of 73 bioactive substances consisting of the plants and drug compounds. Subsequently, the performance of 26 empirical models in predicting the solubility of the bioactive substances in binary mixtures (solute+SC—CO₂) are evaluated accordingly.

2.1. Density-based empirical models

A total of 26 empirical models were employed to correlate the solubility of 73 bioactive compounds (33 drugs and 40 plants) in SC—CO₂ after which their performances were assessed based on the computed absolute average relative deviation (AARD). These 73 bioactive compounds selected for this study are common drug- and plant-based bioactive compounds. Besides, as mentioned, less work was performed on the solubility studies, thus the solubility data in binary SC—CO₂ system might not be readily available for some bioactive compounds. These 73 bioactive compounds were chosen as their solubility data was completely available at diverse operating conditions (pressure and temperature). Majority of the solubility data used in this study were compiled from the publications in the last decade. Unlike other solubility modeling studies, the bioactive compounds considered in this study is not only limited to drugs but also plant-based bioactive compounds.

The 26 models can be sub-classified according to the number of parameters present in the equation (3, 4, 5, 6, and 8-parameter models). Table 1 shows 26 equations found in literature that are arranged in chronological order of its introduction for solubility measurement. As presented in Table 1, y_1 represents the solubility mole fraction of a bioactive compound, ρ represents the density of the supercritical fluid at a given operating condition in cubic metres (kg/m³), T represents the temperature in Kelvin (K), while P represents the pressure in Mega Pascal (MPa).

Adjusted parameters **a - h** of all the 26 density-based models were obtained by regressing the experimental solubility data of individual bioactive compound compiled from its corresponding literature. This was carried out using the solver feature of Microsoft Excel's Regression function under the Data Analysis tool pack. The squared difference between the literature experimental data and the predicted solubility from the models was selected using the least squares regression method

Table 3
Solubility data of drug-based bioactive compounds in binary SC-CO₂ system.

No.	Extracted product	Temperature (K)	Pressure (MPa)	Solubility (mol/mol)	
				min	max
1	Atropine ^a	308 - 348	12.2 - 35.5	6.00 × 10 ⁻⁵	1.67 × 10 ⁻³
2	Codeine ^a	308 - 348	12.2 - 35.5	4.00 × 10 ⁻⁵	1.23 × 10 ⁻³
3	Tridodecylamine ^b	308 - 328	8.0 - 40.0	8.00 × 10 ⁻⁵	1.13 × 10 ⁻²
4	Cefuroxime Axetil ^c	308 - 328	8.0 - 25.0	2.20 × 10 ⁻⁷	1.12 × 10 ⁻⁵
5	Warfarin ^d	308.2 - 328.2	10.0 - 18.0	1.08 × 10 ⁻⁶	5.39 × 10 ⁻⁶
6	Aprepitant ^e	308.15 - 338.15	12.0 - 33.0	4.50 × 10 ⁻⁶	7.67 × 10 ⁻⁵
7	Loratadine ^f	308.15 - 338.15	12.0 - 27.0	4.50 × 10 ⁻⁶	1.30 × 10 ⁻³
8	Aspirin ^g	298.2 - 353.2	7.5 - 35.0	1.95 × 10 ⁻⁵	1.99 × 10 ⁻²
9	Letrozole ^h	318.2 - 348.2	12.0 - 36.0	1.60 × 10 ⁻⁶	8.51 × 10 ⁻⁵
10	Amiodarone Hydrochloride (AMH) ⁱ	313.2 - 343.2	12.0 - 30.0	2.51 × 10 ⁻⁵	1.01 × 10 ⁻³
11	Benzamide ^j	308.15 - 328.15	11.0 - 21.0	1.91 × 10 ⁻⁵	1.61 × 10 ⁻⁴
12	Ketoprofen ^k	308.15 - 338.15	16.0 - 40.0	2.21 × 10 ⁻⁵	7.12 × 10 ⁻⁴
13	Diclofenac Acid ^l	308.15 - 338.15	12.0 - 40.0	2.34 × 10 ⁻⁵	1.98 × 10 ⁻³
14	Gabapentin ^m	308 - 338	16.0 - 40.0	8.97 × 10 ⁻⁵	7.36 × 10 ⁻³
15	Niflumic acid ⁿ	313.2 - 353.2	19.0 - 31.0	7.10 × 10 ⁻⁶	2.09 × 10 ⁻⁵
16	d-Pinitol ^o	313.15 - 333.15	10.0 - 40.0	5.65 × 10 ⁻⁶	8.32 × 10 ⁻⁴
17	Imatinib Mesylate ^p	308 - 338	12.0 - 27.0	1.00 × 10 ⁻⁷	4.41 × 10 ⁻⁶
18	Sorafenib Tosylate ^q	308 - 338	12.0 - 27.0	6.80 × 10 ⁻⁷	1.26 × 10 ⁻⁵
19	Sunitinib Mesylate ^r	308 - 338	12.0 - 27.0	5.00 × 10 ⁻⁶	8.56 × 10 ⁻⁵
20	Repaglinide Drug ^s	308 - 338	12.0 - 27.0	2.90 × 10 ⁻⁶	9.52 × 10 ⁻⁵
21	Azathioprine ^t	308 - 338	12.0 - 27.0	2.70 × 10 ⁻⁶	1.83 × 10 ⁻⁵
22	Sodium Valproate ^u	308 - 338	12.0 - 27.0	5.00 × 10 ⁻⁷	3.71 × 10 ⁻⁵
23	Flurbiprofen ^v	303 - 323	8.9 - 24.5	1.67 × 10 ⁻⁵	1.97 × 10 ⁻⁴
24	Megestrol acetate ^w	308 - 338	12.2 - 35.5	2.90 × 10 ⁻⁶	8.71 × 10 ⁻⁵

Table 3 (continued)

No.	Extracted product	Temperature (K)	Pressure (MPa)	Solubility (mol/mol)	
				min	max
25	Esomeprazole (ESM) ^x	308.2 - 338.	12.0 - 27.0	1.10 × 10 ⁻⁵	9.10 × 10 ⁻⁴
26	2,3,5,6-Tetrachloropyridine ^y	313.2 - 333.2	10.0 - 24.0	3.50 × 10 ⁻⁴	1.09 × 10 ⁻²
27	Chloropropamide ^z	313.2 - 353.2	10.0 - 30.0	2.29 × 10 ⁻⁶	7.22 × 10 ⁻⁵
28	Tolbutamide ^z	313.2 - 353.2	10.0 - 30.0	1.66 × 10 ⁻⁵	4.05 × 10 ⁻⁴
29	Thioxanthone (T1) ^{z1}	308 - 338	12.1 - 35.4	1.00 × 10 ⁻⁶	1.58 × 10 ⁻⁴
30	1-hydroxythioxanthone (T2) ^{z1}	308 - 338	12.1 - 35.5	3.30 × 10 ⁻⁵	4.24 × 10 ⁻⁴
31	3-methylthioxanthone (T3) ^{z1}	308 - 338	12.1 - 35.6	3.60 × 10 ⁻⁵	3.18 × 10 ⁻⁴
32	1,4-dihydroxy-3-methylthioxanthone (T4) ^{z1}	308 - 338	12.1 - 35.7	2.80 × 10 ⁻³	4.31 × 10 ⁻⁵
33	Sertraline Hydrochloride ^{z2}	308-338	12 - 30	1.00 × 10 ⁻⁶	9.30 × 10 ⁻⁵

^a [101],

^b [43],

^c [63],

^d [17],

^e [93],

^f [89],

^g [36],

^h [34],

ⁱ [94],

^j [50],

^k [71],

^l [104],

^m [76],

ⁿ [99],

^o [14],

^p [87],

^q [88],

^r [86],

^s [84],

^t [85],

^u [90,91],

^v [24],

^w [102],

^x [82],

^y [20],

^z [53],

^{z1} [75],

^{z2} [92].

combined with the solver function of Microsoft Excel. The solver function would determine the values of those adjusted parameters when the squared sums for each iteration were at their minimum.

As noticed from Table 1, when presented in chronological order, it is evident that the density-based models developed in the recent years no longer incorporate pressure in the equations as they tend to result in poor correlation of the solubility data [12]. Table 2 shows the density-based models categorized according to their number of model parameters.

A study conducted by many researchers have concluded that models with greater number of parameters result in higher accuracy [12,26,79]. Therefore, this work also aims to evaluate the performance of the 26

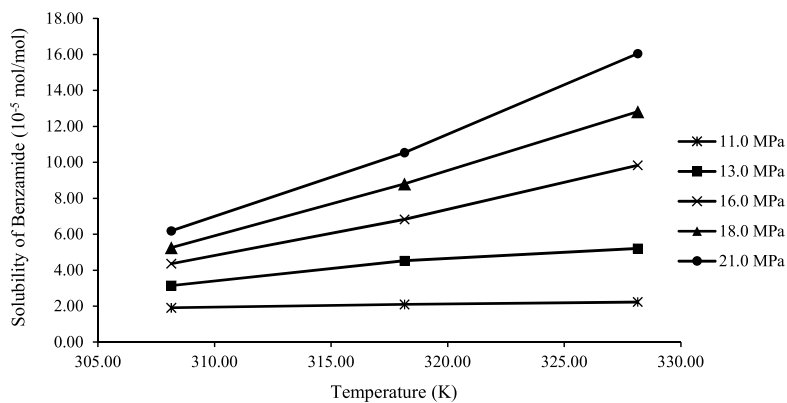


Fig. 2. Effects of Pressure on Solubility of Benzamide [50].

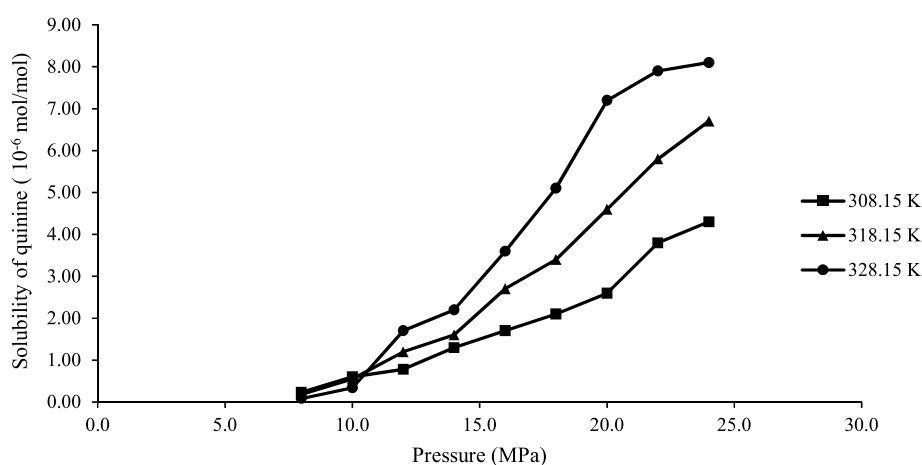
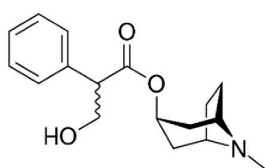


Fig. 3. Effect of Temperature on the Solubility of Quinine [103].



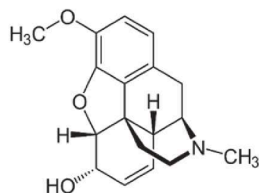
Atropine

289.369 g/mol

Solubility:

4.30×10^{-4} mol/mol

Complexity: 434



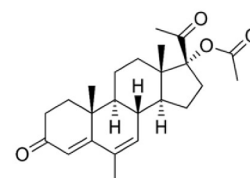
Codeine

299.364 g/mol

Solubility:

3.40×10^{-4} mol/mol

Complexity: 509



Megestrol acetate

342.472 g/mol

Solubility:

4.51×10^{-4} mol/mol

Complexity: 821

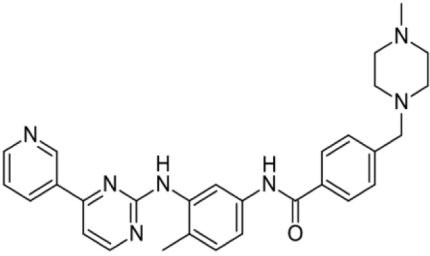
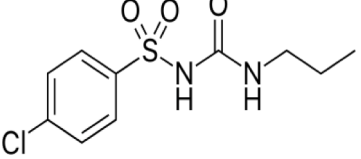
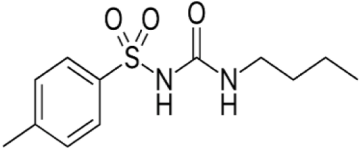
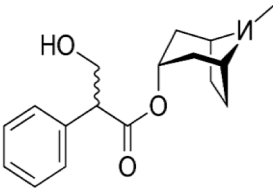
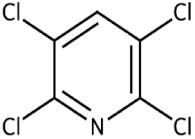
Fig. 4. Molecular structure of Atropine, Codeine, and Megestrol Acetate.

models found in Table 1 with respect to the number of parameters each model contains. The AARD was computed based on Eq. (25) below:

$$AARD (\%) = \left(\frac{100}{n} \right) \sum_{i=1}^n \frac{|y_{exp} - y_{calc}|}{y_{exp}} \quad (25)$$

Where n refers to the number of data points, y_{exp} refers to the experimental solubility, and y_{calc} refers to the calculated solubility using the density-based model.

Table 4
Solubility of major bioactive compounds at approximately 348 K and 25 MPa

Molecular Structure	Solubility Details
<div style="background-color: #808080; color: white; padding: 10px; text-align: center; font-weight: bold;">Minimum solubility</div> 	<p>Imatinib Mesylate Molecular weight = 589.70 g/mol Computed complexity^a = 799 Solubility = 1.76×10^{-6} mol/mol</p>
<div style="background-color: #808080; color: white; padding: 10px; text-align: center; font-weight: bold;">1st Quartile</div> 	<p>Chlorpropamide Molecular weight = 276.74 g/mol Computed complexity^a = 345 Solubility = 2.98×10^{-5} mol/mol</p>
<div style="background-color: #808080; color: white; padding: 10px; text-align: center; font-weight: bold;">Median</div> 	<p>Tolbutamide Molecular weight = 270.35 g/mol Computed complexity^a = 354 Solubility = 1.59×10^{-4} mol/mol</p>
<div style="background-color: #808080; color: white; padding: 10px; text-align: center; font-weight: bold;">3rd Quartile</div> 	<p>Atropine Molecular weight = 289.37 g/mol Computed complexity^a = 353 Solubility = 4.30×10^{-4} mol/mol</p>
<div style="background-color: #808080; color: white; padding: 10px; text-align: center; font-weight: bold;">Maximum Solubility</div> 	<p>2,3,5,6-Tetrachloropyridine Molecular weight = 216.90 g/mol Computed complexity^a = 108 Solubility = 7.28×10^{-3} mol/mol</p>

^a Computed complexity was obtained from <https://pubchem.ncbi.nlm.nih.gov/>

3. Results and discussion

3.1. Solubility-influencing factors

The solubility data of 73 bioactive compounds, comprising of approximately 1500 data points, accompanied by its operating conditions and category were gathered and presented in Tables 3 and 5. Solubility of any given solute is mainly governed by the pressure and temperature of a supercritical system. Continuous tuning of pressure and temperature alters the density and subsequently the solvating power of the supercritical solvent. At isothermal conditions, a rise in pressure enhances the solubility as seen in most supercritical systems [5,6,26,39,50]. Fig. 2 is a clear depiction of how pressure distinctly influences solubility of a given bioactive compound at three different temperatures (308.15 K, 318.15 K, 328.15 K).

However, variation in the operating temperature demands a more sophisticated evaluation as it depends on whether the effects of solute vapor pressure or density is more prevalent. Consequently, a phenomenon known as retrogradation exists alongside a crossover pressure point and is valid for most supercritical systems [5,19,45,103]. Temperature increment beyond crossover point boosts solubility, as the positive effect of solute vapor pressure is more dominant relative to the inverse relationship between pressure and density. Conversely, temperature increment below crossover pressure point gives way to the

negative effects of density relative to the increasing solute vapor pressure, which results in a decline of the solubility. For example, as portrayed in Fig. 3, the crossover pressure is approximately 11.0 MPa. As such, for any increase in temperatures beyond 11.0 MPa, the positive relationship between solute vapor pressure and temperature promotes solubility. On the contrary, temperature rise below 11.0 MPa leads to a reduction in solubility due to a decreasing density.

Besides temperature and pressure, the complexity in the molecular structure of the compound is also an additional factor that governs the solubility of a bioactive compound. A quantitative comparison carried out on the solubility of the bioactive compounds at approximately 328 K and 24 MPa resulted in a hypothetical conclusion that a solute with greater complexity lowers its solubility in supercritical systems. Furthermore, when a solubility comparison was made between Atropine, Codeine, and Megestrol Acetate at 328 K and 24.3 MPa, Atropine, which has the lowest molecular weight and complexity, reported the highest solubility, followed by codeine, and Megestrol acetate [101, 102]. As illustrated in Fig. 4, Atropine possesses only 1 Benzene ring, Codeine has 1 Benzene ring and 3 cyclic groups, whereas Megestrol acetate has several polar C=O bonds in addition to 4 cyclic rings. Hypothetically, the polarity of supercritical carbon dioxide is insufficient in solubilizing relatively more polar solutes [61]. As a matter of fact, in such circumstances, polarity of the solute is also an additional factor that influences a solute's solubility in SFT systems. In studying the solubility

Table 5
Solubility data of plant-based bioactive compounds in binary SC-CO₂ system.

No.	Extracted product	Temperature (K)	Pressure (MPa)	Solubility (mol/mol)	
				min	max
1	Apple seed oil ^{z2}	316 - 336	30.0 - 100.0	3.20 × 10 ⁻³	1.43 × 10 ⁻¹
2	Apricot Kernel Oil ^{z3}	313.15 - 333.15	15.0 - 60.0	1.50 × 10 ⁻²	6.00 × 10 ⁻²
3	Sinapic acid ^{aa}	313 - 333	20.0 - 40.0	7.00 × 10 ⁻⁹	7.04 × 10 ⁻⁷
4	Chrysin ^{aa}	313 - 333	20.0 - 40.0	1.80 × 10 ⁻⁸	1.13 × 10 ⁻⁷
5	Vitamin E Acetate ^{ab}	308.15 - 328.15	8.41 - 14.19	8.41 × 10 ⁻⁴	1.42 × 10 ⁻³
6	Theobromine ^{ac}	313.15 - 353.15	21.9 - 34.5	8.80 × 10 ⁻⁷	4.71 × 10 ⁻⁶
7	Theophylline ^{ac}	313.15 - 353.15	19.9 - 34.9	1.03 × 10 ⁻⁵	3.32 × 10 ⁻⁵
8	Hemp Seed Oil ^{ad}	313 - 353	20.0 - 40.0	2.90 × 10 ⁻³	3.26 × 10 ⁻²
9	Beta Karotene ^{ae}	313 - 353	20.0 - 35.0	2.90 × 10 ⁻⁴	3.56 × 10 ⁻³
10	Castor Oil ^{af}	313 - 353	20.0 - 36.0	1.00 × 10 ⁻³	4.88 × 10 ⁻³
11	Red Pepper Oil ^{ag}	303 - 333	10.0 - 35.0	1.80 × 10 ⁻⁷	1.18 × 10 ⁻⁶
12	Quinine ^{ah}	308.15 - 328.15	8.0 - 24.0	8.30 × 10 ⁻⁸	8.10 × 10 ⁻⁶
13	Cinnamic acid ^{ai}	308 - 328	9.0 - 18.0	2.78 × 10 ⁻⁵	1.64 × 10 ⁻⁴
14	Clove Oil (spice) ^{aj}	305 - 320	9.0 - 25.0	2.30 × 10 ⁻¹	2.90 × 10 ⁻¹
15	Caffeine ^{ac}	313.15 - 353.15	19.9 - 34.9	2.83 × 10 ⁻⁴	1.13 × 10 ⁻³
16	Green Coffee Oil ^{ak}	313.15 - 353.15	30.0 - 35.0	1.24 × 10 ⁻²	2.60 × 10 ⁻²
17	Maleic Acid ^{al}	318.15 - 348.15	7.0 - 30.0	1.30 × 10 ⁻⁵	5.59 × 10 ⁻²
18	Vitamin K1 ^{am}	313 - 353	20.0 - 35.0	2.90 × 10 ⁻⁴	3.56 × 10 ⁻³
19	Moringa Oleifera Oil ^{an}	333 - 373	20.0 - 50.0	6.40 × 10 ⁻⁴	1.27 × 10 ⁻²
20	Protocatechuic acid ^{ao}	313 - 333	20.0 - 40.0	1.52 × 10 ⁻⁷	1.06 × 10 ⁻⁶
21	Palm Kernel Shell (bio-oil) ^{ap}	323 - 343	30.0 - 40.0	4.56 × 10 ⁻⁴	1.04 × 10 ⁻³
22	Passion Fruit seed oil ^{aq}	313 - 333	20.0 - 25.0	1.81 × 10 ⁻³	5.52 × 10 ⁻³
23	Arachis Hypogea Skin (Peanut) Oil ^{ar}	313 - 343	10.0 - 30.0	1.28 × 10 ⁻³	2.22 × 10 ⁻³
24	Paeonol ^{at}	313.2 - 333.2	8.6 - 14.3	2.79 × 10 ⁻³	1.00 × 10 ⁻¹

Table 5 (continued)

No.	Extracted product	Temperature (K)	Pressure (MPa)	Solubility (mol/mol)	
				min	max
25	Vitamin D2 ^{am}	313 - 353	20.0 - 32.0	2.90 × 10 ⁻⁴	1.04 × 10 ⁻³
26	Pomegranate seed oil ^{as}	313 - 333	24.0 - 32.00	9.70 × 10 ⁻⁴	2.04 × 10 ⁻³
27	Mesquite Gum ^{at}	313 - 343	13.8 - 34.5	2.62 × 10 ⁻⁹	1.19 × 10 ⁻⁸
28	Vitamin E (γ) ^{am}	313 - 353	19.9 - 34.9	6.40 × 10 ⁻⁴	3.57 × 10 ⁻³
29	Red Palm Oil ^{au}	313.15 - 333.15	8.7 - 25.2	5.30 × 10 ⁻⁴	1.13 × 10 ⁻²
31	Roselle seed oil ^{av}	313 - 353	20.0 - 30.0	5.80 × 10 ⁻⁴	1.07 × 10 ⁻³
32	Oleic acid ^{aw}	313.15 - 353.15	10.0 - 30.00	3.80 × 10 ⁻⁶	2.24 × 10 ⁻³
33	Sunflower Oil ^{ax}	313 - 353	20.0 - 35.0	2.00 × 10 ⁻⁴	9.90 × 10 ⁻³
34	Curcumin ^{ay}	308 - 328	8.0 - 20.0	1.82 × 10 ⁻⁸	3.70 × 10 ⁻⁸
35	Vanillin ^{az}	315 - 334.71	8.6 - 30.1	6.30 × 10 ⁻⁵	5.22 × 10 ⁻³
36	Vitamin E (α) ^{am}	313 - 353	19.9 - 34.9	6.40 × 10 ⁻⁴	3.57 × 10 ⁻³
37	Laminarin ^{ba}	308.15 - 318.15	10 - 16	1.82 × 10 ⁻⁴	3.41 × 10 ⁻⁴
38	Phosphatidylcholine ^{bb}	313 - 353	12.4 - 17.2	5.08 × 10 ⁻⁶	1.18 × 10 ⁻⁵
39	Quercus infectoria (oak) ^{bc}	323 - 343	20 - 30	2.87 × 10 ⁻³	5.22 × 10 ⁻³
40	Black Pepper Piperine ^{bd}	293 - 333	10 - 20	7.80 × 10 ⁻⁶	1.42 × 10 ⁻⁴

z2 [57],

z3 [64],

aa [65],

ab [31],

ac [40],

ad [98],

ae [55],

af [21],

ag [48],

ah [103],

ai [30],

aj [100],

ac [45],

ak [18],

al [72],

am [41],

an [107],

ao [15],

ap [23],

aq [67],

ar [39],

as [59],

at [19],

au [49],

av [66],

aw [4],

ax [78],
 ay [105],
 az [70],
 ba [106],
 bb [38],
 bc [56],
 bd [47].

of solutes in SC-CO₂, more often than not, the amount of hydrogen bonds that can be formed between SC-CO₂ and the solute indirectly dictates the solubility [25]. A study by Antonie and Pereira [8] too, reported these similar findings. The results of the quantitative comparison are tabulated in Table 4, where the bioactive compounds are statistically arranged in order of increasing solubility from the lowest solubility, 1st quartile, median, 3rd quartile, to maximum solubility.

Similar analysis was performed on selected plant-based bioactive compounds listed in Table 4 to study the effect of molecular structure on their solubility. With reference to the maximum solubility data of three phenolic compounds at 333 K and 40.0 MPa adapted from Paula et al. [65] and as shown in Table 5, sinapic acid has the lowest solubility, followed by chrysin, and protocatechuic acid. When a comparison was made to the molecular weight and structure of sinapic acid and protocatechuic acid, it is plausible that sinapic acid has a much lower solubility as opposed to protocatechuic acid. From a molecular weight perspective, sinapic acid is heavier than protocatechuic acid. In the context of molecular structure, two methoxy groups (O-CH₃), 1 hydroxyl (OH) group and one carboxyl (R-COOH) group surrounds the benzene ring of sinapic acid, giving rise to a more complex and bulky structure. Protocatechuic acid, on the other hand, is relatively smaller and simpler with only 2 hydroxyl and 1 carboxylic acid group branching out of its benzene ring as seen in Fig. 5. This indirectly suggests that compounds with a greater overall volume tends to have lower solubility [68].

3.2. Quantitative evaluation and empirical model comparison

As previously specified in Section 2.1, the solubility data of each bioactive compound in a binary supercritical system were regressed to obtain the adjusted parameters for the 26 empirical model equations. The correlation of solubility data with respect to the adjusted model parameters resulted in a computed AARD for each bioactive compound. With reference to Table 6, the lowest AARD for each bioactive compound is marked in bold, indicating the best-performing empirical model with respect to that bioactive compound. Analysing from an overall perspective, the Belghait et al. model (8-parameter model) resulted in the lowest AARD (%) of 7.42 %, 10.16 %, and 6.57 %,

respectively for all bioactive compounds, drug-based bioactive compounds, and plant-based bioactive compounds. Belghait et al. model is also superior since its predictive performances are the best for 54 % of the bioactive compounds studied. When the model was first proposed by Belghait et al. [12], the performance of the model was tested based on the solubility correlation of 210 drug-based compounds and compared against 21 commonly-used density-based equations. In an identical comparative study of empirical models with respect to the solubility of pharmaceutical compounds conducted by Reddy and Garlapati [69], the Belghait et al. model again, emerged as the best performing model. Hence, the results obtained in this study further reaffirm and trumpet the superiority of the Belghait et al. model. Notably, the second-best overall model that is able to predict the solubility of both plant- and drug-based solutes is the 6-parameter Jouyban model, achieving lowest AARD (%) of 12 % for the compounds studied. From these findings, the accuracy of the correlation is hypothetically affected by the number of parameters in the correlation. Besides, it is worth noting that the Modified Chrastil Model (2), as presented in Table 2 as Equation 15(a) has the exact same mathematical formula as that of the Bian model, therefore resulting in the same computed AARD. Due to the aforementioned reason, the numerical AARD figures for Modified Chrastil Model (2) are not tabulated in Tables 6, 7, and 8.

To the best of knowledge, a comprehensive comparative study pertaining the performance of the empirical models on both plant- and drug-based solutes are scarce, as majority are aimed at drugs for instance in these references [9,12,37]. In a recent work carried out by Antonie and Pereira [8], a similar approach was taken in analysing, nevertheless, only a limited number of compounds were compared and the respective AARD computed was obtained from only 4 models [8].

In addition to analysing the performance of all 26 models as a whole, the effectiveness of the models is gauged according to the number of parameters (3, 4, 5, and 6) presented in the equation. The results of the evaluation are presented and segregated according to drug- (Table 7) and plant- (Table 8) based bioactive compounds. For both plant- and drug-based compounds, a consistency in results can be observed where Kumar and Johnston model, Sung and Shim model, as well as Moussa et al. model best-correlated the solubility data among all 3, 4, and 6-parameter models, respectively. Moreover, the satisfactory performance of the Jouyban as a 6-parameter model in this study showed consistency with the results attained by Belghait et al. [12] and Sodeifian, Arbab Nooshabadi, et al. [81]. However, it is worth noting the difference in the results for the 5-parameter models. For drug-based compounds, Adachi and Lu model was able to best correlate the solubility data, whereas Keshmiri et al. model resulted in the lowest overall AARD for plant-based compounds. Similar results were attained in the

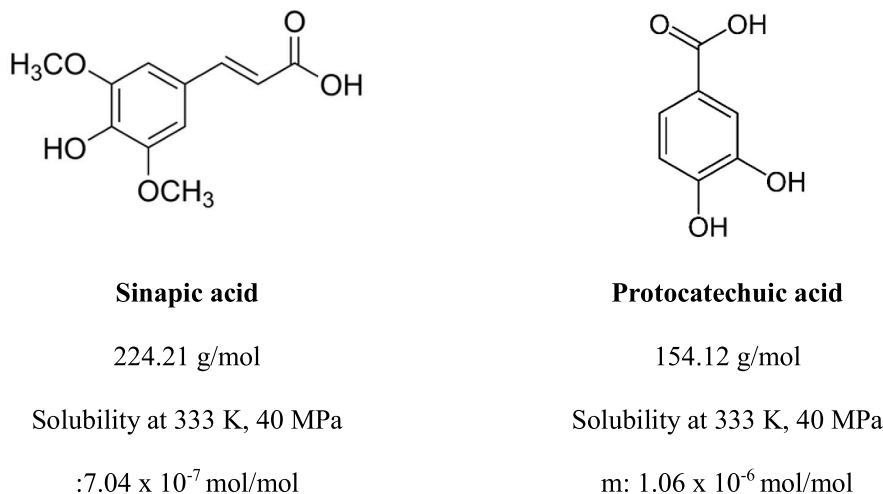


Fig. 5. Molecular structure and solubility data of Sinapic acid and Protocatechuic acid at 333 K and 40 MPa.

Table 7 (continued)

Bioactive compound	Empirical model equation																								
	1	2	3	4	5	6	7	8	9	10	11	12	13	14	15	16	17	18	19	20	21	22	23	24	25 ¹
Tolbutamide	6.91	15.12	9.69	7.07	14.94	8.68	6.51	5.48	4.25	8.84	6.39	9.32	13.23	6.17	4.18	6.17	3.02	3.90	2.79	10.30	14.75	7.84	6.14	2.32	2.31
Cefuroxime Axetil	64.81	64.70	64.57	64.83	49.70	40.15	63.77	28.16	64.15	18.90	28.43	23.53	18.93	27.81	22.33	20.02	21.96	14.47	18.69	14.41	14.31	15.55	19.90	16.27	14.42
Imatinib Mesylate	43.81	42.05	42.72	43.75	36.61	32.56	42.94	33.42	41.96	28.63	30.77	21.29	29.09	31.14	28.06	30.77	18.18	24.56	18.30	8.89	18.82	15.30	31.13	24.02	21.12
Sorafenib Tosylate	14.14	15.62	16.61	14.15	9.24	13.07	13.90	8.21	11.44	8.43	8.44	11.83	8.72	6.75	8.24	8.48	10.22	8.36	8.28	6.65	10.46	10.08	6.74	8.85	5.75
Sunitinib Mesylate	19.87	24.43	25.33	19.90	17.60	20.72	19.40	9.40	15.60	12.65	14.65	16.83	9.50	14.48	13.74	13.70	15.16	8.10	13.45	9.12	7.09	9.41	12.41	14.60	10.93
ESM	11.64	13.40	14.33	11.60	14.98	15.64	11.38	14.74	10.18	13.92	11.60	11.30	13.28	11.45	9.16	10.42	9.96	12.37	9.97	20.87	10.07	9.52	10.15	9.45	7.98
Repaglinide Drug	19.85	17.08	17.25	19.68	13.56	14.18	19.15	13.64	18.42	12.73	12.36	11.33	13.37	12.53	10.76	12.54	11.65	13.31	9.57	11.23	11.43	8.99	12.64	9.71	8.77
Serrraline Hydrochloride	16.33	16.38	15.38	16.35	15.45	15.29	16.45	12.37	16.27	14.80	14.00	11.75	16.37	14.00	11.17	13.91	9.69	10.90	8.86	18.60	19.82	6.28	13.96	10.42	8.41
Azathioprine	6.23	7.06	8.49	6.16	6.72	9.51	5.25	6.18	5.00	5.94	5.65	5.09	5.46	5.20	4.88	5.52	5.10	6.59	5.08	11.30	5.14	7.28	5.31	4.95	4.72
Sodium Valproate	7.34	8.22	9.25	7.34	10.89	11.51	7.14	9.48	6.67	8.70	6.92	6.31	8.37	6.82	6.48	5.69	6.48	8.49	6.25	17.56	5.72	6.50	5.64	5.69	5.39
Average AARD	19.97	21.43	21.70	20.10	18.26	18.17	19.61	13.97	16.98	13.29	13.68	14.39	13.46	12.87	12.38	12.84	12.48	15.69	11.29	16.46	17.28	12.47	12.16	11.64	10.16
MIN AARD	2.60	4.46	2.87	2.83	4.45	1.41	1.42	2.72	1.17	2.28	2.39	3.62	1.93	1.17	1.05	1.91	0.93	1.87	1.06	2.52	2.66	3.21	1.18	0.86	0.86
MAX AARD	120.96	139.18	142.09	120.95	96.30	61.59	124.20	41.05	75.03	43.06	39.79	47.18	41.56	35.82	40.13	43.99	44.36	74.82	44.21	57.83	66.10	51.87	40.80	40.73	38.88
Number of Parameters	3	3	3	3	3	4	4	4	4	4	4	4	4	5	5	5	5	5	6	6	6	6	6	6	8

¹ Comparison is inapplicable as there is only one 8-parameter empirical model

study by Belghait et al. whereby amongst all the 5-parameter models, Adachi and Lu model demonstrated outstanding performance in correlating the data of 210 drug-based compounds [12,77]. Fig. 6 shows the AARD obtained from both Adachi and Lu model, and Keshmiri et al. model for plant-based bioactive compounds. The value of the x-axis of Fig. 6 corresponds to the number of sequences of plant-based bioactive compounds listed in Table 5. As showed in Fig. 6, there is only a minor difference the AARD (%) difference computed between Adachi and Lu model, and Keshmiri et al. model.

As observed from Table 7, the lowest AARD of 0.86 % is attained from both Moussa et al. model (6-parameter model) and Belghait et al. model (8-parameter model). The highest AARD of 64.81 % is found from the use of Chrastil Equation (3-parameter model). While for plant-based bioactive compound, the adoption of both Ch and Madras (4-parameter model) and Garlapati and Madras (II) (5-parameter model) results in the minimum AARD of 0.00 %. The maximum AARD of 60.33 % is computed when Moussa et al. model (6-parameter model) is utilized. From the AARD results shown in Tables 7 and 8 for drug- and plant-based bioactive compounds, it can be affirmed that the type of compound is not a deciding factor for the range of AARD computed. In addition, there is no specific correlation that best fits all compounds.

By summarizing minimum and maximum of%AARD for each drug- and plant-based bioactive compound in Tables 9–10 and further analyze them, it is more apparent that no model works perfectly well for all bioactive compounds. Generally, the solubility model possesses high predictive accuracy when it has more model parameters and each bioactive compound has its own reliable solubility predictive model. Nonetheless, considering molecular complexity and weight, and polarity of the respective bioactive compound, hypothetically, they can also be the influencing factors for the model predictive performance. For example, by benchmarking d-pinitol (complexity: 158, molecular weight: 194.18 g/mol) and vitamin E acetate (complexity: 602, MW: 472.7 g/mol) [58], it is evident from Tables 7 to 10, that for all models, predictive accuracies for d-pinitol solubility seems to be consistently poorer in comparison to vitamin E acetate solubility prediction. Therefore, there may be identified patterns that the models presumably perform better for compounds having higher molecular complexities and weights. On the perspective of bioactive compound polarity, vitamin E acetate, maleic acid, and d-Pinitol have topological polar surface areas of 35.5 Ångströms², 74.6 Ångströms², and 110 Ångströms², respectively [58]. The above data demonstrated that predictive solubility models overall work better with compounds having lower polarity. These phenomena are likely to be consistent with the fact that supercritical CO₂ is non-polar solvent [54] and it will only be effective to dissolve non-polar or less polar compounds.

4. Conclusions

Solubility data compilation of a total of 33 drugs and 40 plant-based bioactive compounds in supercritical carbon dioxide was correlated according to 26 commonly-used density-based models. The influence of temperature, pressure, and structural complexity on the solubility of the bioactive compounds were thoroughly discussed and evaluated. Findings include a stronger influence of molecular complexity as opposed to molecular weight on the solubility of these solutes in a supercritical system. It should be highlighted that literature pertaining to a comprehensive solubility review on both plant- and drug-based compounds are scarce. The performance of 26 empirical models were gauged in accordance with the computed AARD when the solubility data gathered from the past 25 years (1994 – 2019) were correlated, and the adjusted parameters determined. Comparison work resulted in the 8-parameter Belghait et al. model correlating the solubility data the best as it was able to compute lowest AARD (%) for majority of the bioactive compounds considered.

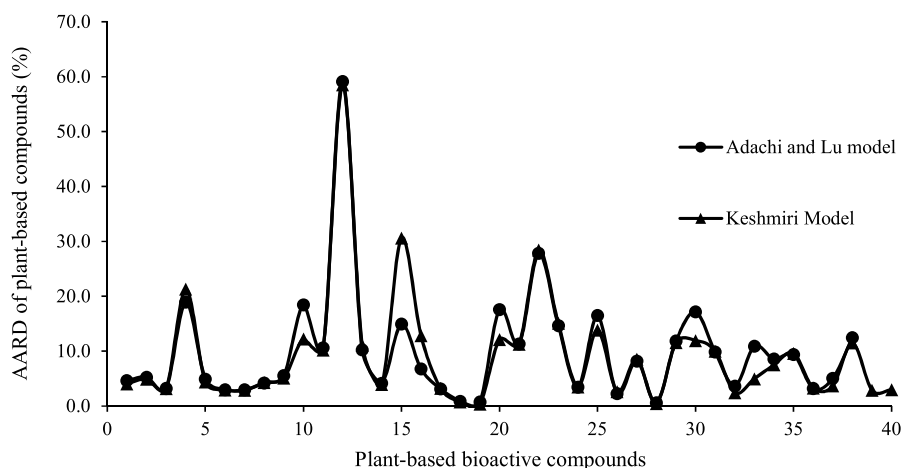


Fig. 6. Graphical representation of the difference between AARD of Adachi and Lu Model and Keshmiri Model.

Table 9

Minimum and maximum AARD for drug-based bioactive compounds.

Drug compound	MIN AARD (%)	MODEL	MAX AARD (%)	MODEL
Atropine	12.56	Belghait	20.41	Nejad
Codeine	7.89	Jouyban	20.07	Khansary
T1	11.96	Sodeifian	31.98	Gordillo
T2	5.23	Jouyban	18.05	Bartle
T3	6.80	Tippana-Garlapati	21.16	Bartle
T4	18.09	Jouyban	28.33	Bartle
Flurbiprofen	6.18	Jouyban	15.65	Bartle
Aspirin	32.42	Del valle Aguilera	57.83	Gordillo
d-Pinitol	22.02	Gordillo	142.09	Bartle
Tridodecylamine	10.88	Belghait	20.41	Nejad
Benzamide	2.37	Belghait	61.59	Modified Chrastil (2)
Ketoprofen	5.34	Keshmiri	13.13	Jouyban
Diclofenac Acid	4.06	Belghait	20.26	Gordillo
Gabapentin	10.23	Belghait	18.76	Tippana-Garlapati
Megestrol acetate	18.96	Khansary	26.02	Bartle
Niflumic acid	0.86	Belghait	5.89	Tippana-Garlapati
2,3,5,6-Tetrachloropyridine	1.93	Hozhabr	20.81	Tippana-Garlapati
Aprepitant	7.58	Belghait	20.71	Chrastil
Amiodarone Hydrochloride	6.20	Jouyban	18.37	Gordillo
Warfarin	2.79	Belghait	18.35	Bartle
Loratadine	10.81	Belghait	31.54	Tippana-Garlapati
Letrozole	3.88	Belghait	26.97	Tippana-Garlapati
Chloropropamide	2.75	Belghait	14.66	Khansary
Toltbutamide	2.31	Belghait	15.12	Mendez-Santiago-Teja
Cefuroxime Axetil	14.31	Tippana-Garlapati	64.83	Garlapati-Madras (i)
Imatinib Mesylate	8.89	Gordillo	43.81	Chrastil
Sorafenib Tosylate	5.75	Belghait	16.61	Bartle
Sutinitib Mesylate	7.09	Tippana-Garlapati	25.33	Bartle
ESM	7.98	Belghait	20.87	Gordillo
Repaglinide Drug	8.77	Belghait	19.85	Chrastil
Sertraline Hydrochloride	6.28	Jouyban	19.82	Tippana-Garlapati
Azathiopine	4.72	Belghait	11.30	Gordillo
Sodium Valproate	5.39	Belghait	17.56	Gordillo

5. Recommendations for future works

To further facilitate the growth of the supercritical fluid industry, future research work with respect to solubility of bioactive compounds is recommended. In terms of solubility-predictive models, the majority of the comparative review were carried out to gauge the performance of density-based models as opposed to the more complex thermodynamic EOS models. In such circumstances, albeit the simplistic nature of the density-based models, it is ideal to carry out comparative studies on both density-based and thermodynamic EOS models. To date, review works on the performance of both models stated are scarce in literature. In

addition, more research can be carried out to analyze the performance of ternary systems, where a co-solvent is added to SC-CO₂. Moreover, as empirical models typically involve temperature, pressure, and density parameters, future research could study the possibility of incorporating the effects of molecular structure and polarity into the predictive modeling equations. Subsequently, this would encourage the use of molecular simulation as a qualitative modeling tool to gain an insight on the effects of molecular structure and polarity towards solubility in the supercritical systems.

Table 10
Minimum and maximum AARD for plant-based bioactive compounds.

Plant-based compound	MIN AARD (%)	MODEL	MAX AARD (%)	MODEL
Theobromine	3.81	Moussa	8.94	Bartle
Theophylline	3.39	Belghait	7.53	Khansary
Caffeine	2.85	Belghait	10.03	Khansary
Vitamin D3	16.72	Belghait	32.60	Tippana-Garlapati
Vitamin D2	3.37	Belghait	21.49	Chrastil
Vitamin E (alpha)	2.64	Belghait	6.81	Khansary
Vitamin E (gamma)	2.83	Belghait	9.01	Khansary
Vitamin K1	3.53	Belghait	8.38	Khansary
Apricot Kernel Oil	1.35	Sodeifian	12.37	Mendez-Santiago-Teja
Sunflower Oil (stearic acid)	5.73	Belghait	23.88	Kumar-Johnston
Black Pepper Piperine	6.71	Belghait	21.14	Chrastil
Maleic Acid	42.79	Garlapati-Madras (ii)	93.03	Modified Chrastil (2)
Red Pepper Oil (linoleic acid)	7.41	Jouyban	24.52	Bartle
Mesquite Gum	2.51	Belghait	6.89	Modified Chrastil (2)
Oleic acid	9.71	Belghait	41.72	Chrastil
Hemp Seed Oil	4.25	Belghait	22.22	Bartle
Moringa Oleifera Oil	1.45	Sparks	8.35	Gordillo
Castor Oil	0.72	Belghait	4.08	Kumar-Johnston
Clove Oil (spice)	0.39	Keshmiri	13.40	Bartle
Vanillin	12.15	Keshmiri	44.78	Modified Chrastil (2)
Chrysin	10.82	Jouyban	16.54	Sung-Shim
Sinapic acid	26.96	Moussa	30.27	Jouyban
Protocatechuic acid	12.58	Jouyban	18.59	Bartle
Palm Kernel Shell (bio-oil)	3.21	Khansary	5.34	Bartle
Quinine	12.24	Belghait	38.56	Modified Chrastil (2)
Curcumin	1.62	Jouyban	11.68	Mendez-Santiago-Teja
Green Coffee Oil	1.76	Belghait	11.80	Mendez-Santiago-Teja
Vitamin E Acetate	0.00	Hozhabr	2.15	Mendez-Santiago-Teja
Apple seed oil	10.94	Belghait	35.10	Khansary
Red Palm Oil	9.77	Jouyban	42.06	Bartle
Arachis Hypogea Skin Oil	4.19	Belghait	16.56	Bartle
Cinnamic acid	1.48	Moussa	11.10	Modified Chrastil (2)
Beta Karotene	4.59	Sodeifian	45.24	Tippana-Garlapati
Paeonol (Peanut oil)	6.82	Belghait	9.46	Mendez-Santiago-Teja
Passion Fruit seed oil	0.60	Belghait	82.92	Jiang
Quercus infectoria (oak)	1.62	Belghait	10.63	Bartle
Pomegranate seed oil	1.25	Gordillo	14.87	Bartle
Roselle seed oil	1.60	Belghait	9.46	Mendez-Santiago-Teja
Laminarin	1.81	Sodeifian	7.89	Bartle
Phosphatidylcholine	0.57	Belghait	9.35	Chrastil

CRediT authorship contribution statement

Christine Ann Obek: Writing – original draft, Validation, Software, Methodology, Investigation, Formal analysis, Data curation, Conceptualization. **Agus Saptoro:** Supervision, Software, Resources, Methodology, Investigation, Funding acquisition, Data curation, Conceptualization. **Angnes Ngieng Tze Tiong:** Writing – review & editing, Supervision. **Zeinab Abbas Jawad:** Writing – original draft, Supervision. **Zong Yang Kong:** Writing – review & editing, Visualization. **Suryadi Ismadji:** Visualization, Supervision, Conceptualization. **Jaka Sunarso:** Writing – review & editing, Supervision.

Declaration of competing interest

The authors declare that they have no known competing financial interests or personal relationships that could have appeared to influence the work reported in this paper.

Data availability

Data will be made available on request.

Acknowledgement

The first author would like to acknowledge the financial support from Curtin University Malaysia under Curtin Malaysia Postgraduate Research Scholarship (CMPRS) to carry out her Ph.D. project.

References

- [1] M. Abadian, G. Sodeifian, F. Razmimanesh, S.Z. Mahmoudabadi, Experimental measurement and thermodynamic modeling of solubility of Riluzole drug (neuroprotective agent) in supercritical carbon dioxide, *Fluid Phase Equilib.* 567 (2023) 113711, <https://doi.org/10.1016/j.fluid.2022.113711>.
- [2] Y. Adachi, B.C.Y. Lu, Supercritical fluid extraction with carbon dioxide and ethylene, *Fluid Phase Equilib.* 14 (1983) 147–156, [https://doi.org/10.1016/0378-3812\(83\)80120-4](https://doi.org/10.1016/0378-3812(83)80120-4).
- [3] H. Ahangari, J.W. King, A. Ehsani, M. Yousefi, Supercritical fluid extraction of seed oils – a short review of current trends, *Trends Food Sci. Technol.* 111 (2021) 249–260, <https://doi.org/10.1016/j.tifs.2021.02.066>.
- [4] N. Al-Darmaki, T. Lu, B. Al-Duri, J.B. Harris, T.L.F. Favre, K. Bhagga, R.C. D. Santos, Solubility measurements and analysis of binary, ternary and quaternary systems of palm olein, squalene and oleic acid in supercritical carbon dioxide, *Sep. Purif. Technol.* 83 (2011) 189–195, <https://doi.org/10.1016/j.seppur.2011.09.043>.
- [5] S.M. Alshahrani, A.M. Alsubaiyel, M.H. Abduljabbar, M.A.S. Abourehab, Measurement of metoprolol solubility in supercritical carbon dioxide; experimental and modeling study, *Case Stud. Therm. Eng.* 42 (2023) 102764, <https://doi.org/10.1016/j.csite.2023.102764>.
- [6] M. Amani, N. Saadati Ardestani, A. Jouyban, S.A. Sajadian, Solubility measurement of the fludrocortisone acetate in supercritical carbon dioxide: experimental and modeling assessments, *J. Supercrit. Fluids* 190 (2022) 105752, <https://doi.org/10.1016/j.supflu.2022.105752>.

- [7] Y.Y. Andrade-Avila, J. Cruz-Olivares, C. Pérez-Alonso, C.H. Ortiz-Estrada, M. C. Chaparro-Mercado, Supercritical extraction process of allspice essential oil, *J. Chem. Eng.* 2017 (2017) 6471684, <https://doi.org/10.1155/2017/6471684>.
- [8] P. Antonie, C.G. Pereira, Solubility of functional compounds in supercritical CO₂: data evaluation and modelling, *J. Food Eng.* 245 (2019) 131–138, <https://doi.org/10.1016/j.jfoodeng.2018.10.012>.
- [9] M. Asgarpour Khansary, F. Amiri, A. Hosseini, A.H. Sani, H. Shahbeig, Representing solute solubility in supercritical carbon dioxide: a novel empirical model, *Chem. Eng. Res. Des.* 93 (2015) 355–365, <https://doi.org/10.1016/j.cherd.2014.05.004>.
- [10] H. Bagheri, B. Notej, S. Shahsavari, H. Hashemipour, Supercritical carbon dioxide utilization in drug delivery: experimental study and modeling of paracetamol solubility, *Eur. J. Pharmaceut. Sci.* 177 (2022) 106273, <https://doi.org/10.1016/j.ejps.2022.106273>.
- [11] K.D. Bartle, A.A. Clifford, S.A. Jafar, G.F. Shilstone, Solubilities of solids and liquids of low volatility in supercritical carbon dioxide, *J. Phys. Chem. Ref. Data* 20 (4) (1991) 713–756, <https://doi.org/10.1063/1.555893>.
- [12] A. Belghait, C. Si-Moussa, M. Laidi, S. Hanini, Semi-empirical correlation of solid solute solubility in supercritical carbon dioxide: comparative study and proposition of a novel density-based model, *Comptes Rendus Chimie* 21 (5) (2018) 494–513, <https://doi.org/10.1016/j.crci.2018.02.006>.
- [13] X.-Q. Bian, Q. Zhang, Z.-M. Du, J. Chen, J.-N. Jaubert, A five-parameter empirical model for correlating the solubility of solid compounds in supercritical carbon dioxide, *Fluid Phase Equilib.* 411 (2016) 74–80, <https://doi.org/10.1016/j.fluid.2015.12.017>.
- [14] A. Cháfer, T. Fornari, R.P. Stateva, A. Berna, d-Pinitol solubility in supercritical CO₂: experimental data and correlation, *J. Chem. Eng. Data* 51 (2) (2006) 612–615, <https://doi.org/10.1021/je0504257>.
- [15] Y.H. Chan, S. Yusup, A.T. Quitain, Y.H. Chai, Y. Uemura, S.K. Loh, Extraction of palm kernel shell derived pyrolysis oil by supercritical carbon dioxide: evaluation and modeling of phenol solubility, *Biomass Bioenergy* 116 (2018) 106–112, <https://doi.org/10.1016/j.biombioe.2018.06.009>.
- [16] J. Chrastil, Solubility of solids and liquids in supercritical gases, *J. Phys. Chem.* 86 (15) (1982) 3016–3021, <https://doi.org/10.1021/j100212a041>.
- [17] J.-M. Ciou, B.-C. Wang, C.-S. Su, J.-J. Liu, M.-T. Sheu, Measurement of solid solubility of warfarin in supercritical carbon dioxide and recrystallization study using supercritical antisolvent process, *Adv. Powder Technol.* 29 (3) (2018) 479–487, <https://doi.org/10.1016/j.apt.2017.12.005>.
- [18] H.P. Cornelio-Santiago, C.B. Gonçalves, N.A. Oliveira, A.L. Oliveira, Supercritical CO₂ extraction of oil from green coffee beans: solubility, triacylglycerol composition, thermophysical properties and thermodynamic modelling, *J. Supercrit. Fluids* 128 (2017) 386–394, <https://doi.org/10.1016/j.supflu.2017.05.030>.
- [19] J. Cruz-Olivares, C.H. Ortiz-Estrada, C. Pérez-Alonso, M.C. Chaparro-Mercado, C. Barrera-Díaz, Solubility of mesquite gum in supercritical carbon dioxide, *J. Chem. Eng. Data* 56 (5) (2011) 2449–2452, <https://doi.org/10.1021/je2000155>.
- [20] H. Cui, S. Qian, F. Qin, C. Wang, Solubility of 2,3,5,6-tetrachloropyridine in supercritical CO₂: measurement and correlation, *J. Chem. Eng. Data* 59 (2) (2014) 269–274, <https://doi.org/10.1021/je400462d>.
- [21] J.M. Danlami, M.A.A. Zaini, A. Arsad, M.A.C. Yunus, Solubility assessment of castor (*Ricinus communis* L) oil in supercritical CO₂ at different temperatures and pressures under dynamic conditions, *Ind. Crops Prod.* 76 (2015) 34–40, <https://doi.org/10.1016/j.indcrop.2015.06.010>.
- [22] J.M. Del Valle, J.M. Aguilera, An improved equation for predicting the solubility of vegetable oils in supercritical carbon dioxide, *Ind. Eng. Chem. Res.* 27 (8) (1988) 1551–1553, <https://doi.org/10.1021/ie00080a036>.
- [23] D. Santos, L. Cristina, R.G. Bitencourt, P. Santos, P.T.V. Rosa, J. Martínez, Solubility of passion fruit (*Passiflora edulis* Sims) seed oil in supercritical CO₂, *Fluid Phase Equilib.* 493 (2019) 174–180, <https://doi.org/10.1016/j.fluid.2019.04.002>.
- [24] A.R.C. Duarte, P. Coimbra, H.C. Sousa, C.M.M. Duarte, Solubility of flurbiprofen in supercritical carbon dioxide, *J. Chem. Eng. Data* 49 (3) (2004) 449–452, <https://doi.org/10.1021/je034099b>.
- [25] C.A. Eckert, B.L. Knutson, Molecular charisma in supercritical fluids, *Fluid Phase Equilib.* 83 (1993) 93–100, [https://doi.org/10.1016/0378-3812\(93\)87011-O](https://doi.org/10.1016/0378-3812(93)87011-O).
- [26] N. Esfandiari, S.A. Sajadian, Solubility of Lacosamide in supercritical carbon dioxide: an experimental analysis and thermodynamic modeling, *J. Mol. Liq.* 360 (2022) 119467, <https://doi.org/10.1016/j.molliq.2022.119467>.
- [27] C. Garlapati, G. Madras, Solubilities of solids in supercritical fluids using dimensionally consistent modified solvate complex models, *Fluid Phase Equilib.* 283 (1) (2009) 97–101, <https://doi.org/10.1016/j.fluid.2009.05.013>.
- [28] C. Garlapati, G. Madras, New empirical expressions to correlate solubilities of solids in supercritical carbon dioxide, *Thermochim. Acta* 500 (1) (2010) 123–127, <https://doi.org/10.1016/j.tca.2009.12.004>.
- [29] M.D. Gordillo, M.A. Blanco, A. Molero, E. Martínez de la Ossa, Solubility of the antibiotic Penicillin G in supercritical carbon dioxide, *J. Supercrit. Fluids* 15 (3) (1999) 183–190, [https://doi.org/10.1016/S0896-8446\(99\)00008-X](https://doi.org/10.1016/S0896-8446(99)00008-X).
- [30] L. Guo, M. Qu, J. Jin, H. Meng, Solubility of cinnamic acid in supercritical carbon dioxide and subcritical 1,1,1,2-tetrafluoroethane: experimental data and modelling, *Fluid Phase Equilib.* 480 (2019) 66–80, <https://doi.org/10.1016/j.fluid.2018.10.009>.
- [31] S. Han, W. Wang, Z. Jiao, X. Wei, Solubility of Vitamin E acetate in supercritical carbon dioxide: measurement and correlation, *J. Chem. Eng. Data* 62 (11) (2017) 3854–3860, <https://doi.org/10.1021/acs.jced.7b00550>.
- [32] J. Hasanov, S. Salikhov, Y. Oshchepkova, Techno-economic evaluation of supercritical fluid extraction of flaxseed oil, *J. Supercrit. Fluids* 194 (2023) 105839, <https://doi.org/10.1016/j.supflu.2023.105839>.
- [33] M. Herrero, J.A. Mendiola, A. Cifuentes, E. Ibáñez, Supercritical fluid extraction: recent advances and applications, *J. Chromatogr. A* 1217 (16) (2010) 2495–2511, <https://doi.org/10.1016/j.chroma.2009.12.019>.
- [34] M. Hojjati, A. Vatanara, Y. Yamini, M. Moradi, A.R. Najafabadi, Supercritical CO₂ and highly selective aromatase inhibitors: experimental solubility and empirical data correlation, *J. Supercrit. Fluids* 50 (3) (2009) 203–209, <https://doi.org/10.1016/j.supflu.2009.06.015>.
- [35] S.B. Hozhabr, S.H. Mazloumi, J. Sargolzaei, Correlation of solute solubility in supercritical carbon dioxide using a new empirical equation, *Chem. Eng. Res. Des.* 92 (11) (2014) 2734–2739, <https://doi.org/10.1016/j.cherd.2014.01.026>.
- [36] Z. Huang, W.D. Lu, S. Kawi, Y.C. Chiew, Solubility of aspirin in supercritical carbon dioxide with and without acetone, *J. Chem. Eng. Data* 49 (5) (2004) 1323–1327, <https://doi.org/10.1021/je0499465>.
- [37] S. Jafari Nejad, H. Abolghasemi, M.A. Moosavian, M.G. Maragheh, Prediction of solute solubility in supercritical carbon dioxide: a novel semi-empirical model, *Chem. Eng. Res. Des.* 88 (7) (2010) 893–898, <https://doi.org/10.1016/j.cherd.2009.12.006>.
- [38] A. Jash, T. Hatami, S.S.H. Rizvi, Phosphatidylcholine solubility in supercritical carbon dioxide: experimental data, thermodynamic modeling, and application in bioactive-encapsulated liposome synthesis, *J. Supercrit. Fluids* 158 (2020) 104720, <https://doi.org/10.1016/j.supflu.2019.104720>.
- [39] Z. Jiao, J. Cheng, M. Guo, S. Han, Measurement and correlation of paeonol solubility in supercritical carbon dioxide, *J. Chem. Eng. Data* 64 (10) (2019) 4424–4429, <https://doi.org/10.1021/acs.jced.9b00483>.
- [40] M. Johannsen, G. Brunner, Solubilities of the xanthines caffeine, theophylline and theobromine in supercritical carbon dioxide, *Fluid Phase Equilib.* 95 (1994) 215–226, [https://doi.org/10.1016/0378-3812\(94\)80070-7](https://doi.org/10.1016/0378-3812(94)80070-7).
- [41] M. Johannsen, G. Brunner, Solubilities of the Fat-Soluble Vitamins A, D, E, and K in supercritical carbon dioxide, *J. Chem. Eng. Data* 42 (1) (1997) 106–111, <https://doi.org/10.1021/je960219m>.
- [42] A. Jouyban, H.-K. Chan, N.R. Foster, Mathematical representation of solute solubility in supercritical carbon dioxide using empirical expressions, *J. Supercrit. Fluids* 24 (1) (2002) 19–35, [https://doi.org/10.1016/S0896-8446\(02\)00015-3](https://doi.org/10.1016/S0896-8446(02)00015-3).
- [43] M. Kaboudvand, H.S. Ghaziaskar, Solubility of tridodecylamine in supercritical carbon dioxide, *J. Chem. Eng. Data* 53 (11) (2008) 2722, <https://doi.org/10.1021/je8007233>.
- [44] K. Keshmiri, A. Vatanara, Y. Yamini, Development and evaluation of a new semi-empirical model for correlation of drug solubility in supercritical CO₂, *Fluid Phase Equilib.* 363 (2014) 18–26, <https://doi.org/10.1016/j.fluid.2013.11.013>.
- [45] U. Kopeck, R.S. Mohamed, Caffeine solubility in supercritical carbon dioxide/cosolvent mixtures, *J. Supercrit. Fluids* 34 (2) (2005) 209–214, <https://doi.org/10.1016/j.supflu.2004.11.016>.
- [46] S.K. Kumar, K.P. Johnston, Modelling the solubility of solids in supercritical fluids with density as the independent variable, *J. Supercrit. Fluids* 1 (1) (1988) 15–22, [https://doi.org/10.1016/0896-8446\(88\)90005-8](https://doi.org/10.1016/0896-8446(88)90005-8).
- [47] A.C. Kumoro, H. Singh, M. Hasan, Solubility of piperine in supercritical and near critical carbon dioxide, *Chin. J. Chem. Eng.* 17 (6) (2009) 1014–1020, [https://doi.org/10.1016/S1004-9541\(08\)60310-9](https://doi.org/10.1016/S1004-9541(08)60310-9).
- [48] K.-T. Kwon, M. Salim Uddin, G.-W. Jung, J.-E. Sim, S.-M. Lee, H.-C. Woo, B.-S. Chun, Solubility of red pepper (*Capsicum annuum*) oil in near- and supercritical carbon dioxide and quantification of capsaicin, *Korean J. Chem. Eng.* 28 (2011) 1433–1438, <https://doi.org/10.1007/s11814-010-0515-x>.
- [49] W.J. Lee, C.P. Tan, R. Sulaiman, G.H. Chong, Solubility of red palm oil in supercritical carbon dioxide: measurement and modelling, *Chin. J. Chem. Eng.* 26 (5) (2018) 964–969, <https://doi.org/10.1016/j.cjche.2017.09.024>.
- [50] J.-L. Li, J.-S. Jin, Z.-T. Zhang, Y.-B. Wang, Measurement and correlation of solubility of benzamide in supercritical carbon dioxide with and without cosolvent, *Fluid Phase Equilib.* 307 (1) (2011) 11–15, <https://doi.org/10.1016/j.fluid.2011.04.021>.
- [51] R.N. Lima, A.S. Ribeiro, L. Cardozo-Filho, D. Vedoy, P.B. Alves, Extraction from leaves of Piper Klotzschianum using supercritical carbon dioxide and co-solvents, *J. Supercrit. Fluids* 147 (2019) 205–212, <https://doi.org/10.1016/j.supflu.2018.11.006>.
- [52] M. Majrashi, A.S. Al-Shati, M. Grishina, S.M. Sarkar, M.-T. Nguyen-Le, S. Shirazian, Experimental measurement and thermodynamic modeling of Chlorothiazide solubility in supercritical carbon dioxide, *Case Stud. Therm. Eng.* 41 (2023) 102621, <https://doi.org/10.1016/j.csite.2022.102621>.
- [53] L. Manna, M. Banchemo, Solubility of tolbutamide and chlorpropamide in supercritical carbon dioxide, *J. Chem. Eng. Data* 63 (5) (2018) 1745–1751, <https://doi.org/10.1021/acs.jced.8b00050>.
- [54] S.D. Manjare, K. Dhingra, Supercritical fluids in separation and purification: a review, *Mater. Sci. Energy Technol.* 2 (3) (2019) 463–484, <https://doi.org/10.1016/j.mset.2019.04.005>.
- [55] R.L. Mendes, B.P. Nobre, J.P. Coelho, A.F. Palavra, Solubility of β -carotene in supercritical carbon dioxide and ethane, *J. Supercrit. Fluids* 16 (2) (1999) 99–106, [https://doi.org/10.1016/S0896-8446\(99\)00029-7](https://doi.org/10.1016/S0896-8446(99)00029-7).

- [56] H. Mohd Nasir, L.M. Salleh, A.R. Ismail, S. Machmudah, Solubility correlation of gall (*Quercus infectoria*) extract in supercritical CO₂ using semi-empirical equations, *Asia Pac. J. Chem. Eng.* 12 (5) (2017) 790–797, <https://doi.org/10.1002/apj.2118>.
- [57] F. Montañés, O.J. Catchpole, S. Tallon, K.A. Mitchell, D. Scott, R.F. Webby, Extraction of apple seed oil by supercritical carbon dioxide at pressures up to 1300 bar, *J. Supercrit. Fluids* 141 (2018) 128–136, <https://doi.org/10.1016/j.supflu.2018.02.002>.
- [58] National Library of Medicine, <https://pubchem.ncbi.nlm.nih.gov/>, retrieved on 31st January 2024.
- [59] A. Natolino, C.D. Porto, Supercritical carbon dioxide extraction of pomegranate (*Punica granatum L.*) seed oil: kinetic modelling and solubility evaluation, *J. Supercrit. Fluids* 151 (2019) 30–39, <https://doi.org/10.1016/j.supflu.2019.05.002>.
- [60] S.J. Nejad, R. Mohammadikhah, H. Abolghasemi, M.A. Moosavian, M. G. Maragheh, A novel equation of state (EOS) for prediction of solute solubility in supercritical carbon dioxide: experimental determination and correlation, *Can. J. Chem. Eng.* 87 (6) (2009) 930–938, <https://doi.org/10.1002/cjce.20232>.
- [61] J. Noroozi, A.S. Paluch, Microscopic structure and solubility predictions of multifunctional solids in supercritical carbon dioxide: a molecular simulation study, *J. Phys. Chem. B* 121 (7) (2017) 1660–1674, <https://doi.org/10.1021/acs.jpcc.6b12390>.
- [62] K.L. Nyam, C.P. Tan, R. Karim, O.M. Lai, K. Long, Y.B.C. Man, Extraction of tocopherol-enriched oils from Kalahari melon and roselle seeds by supercritical fluid extraction (SFE-CO₂), *Food Chem.* 119 (3) (2010) 1278–1283, <https://doi.org/10.1016/j.foodchem.2009.08.007>.
- [63] K. Ongkasin, M. Saucieu, Y. Masmoudi, J. Fages, E. Badens, Solubility of cefuroxime axetil in supercritical CO₂: measurement and modeling, *J. Supercrit. Fluids* 152 (2019) 104498, <https://doi.org/10.1016/j.supflu.2019.03.010>.
- [64] S.G. Özkal, M.E. Yener, L. Bayındır, The solubility of apricot kernel oil in supercritical carbon dioxide, *Int. J. Food Sci. Technol.* 41 (4) (2006) 399–404, <https://doi.org/10.1111/j.1365-2621.2005.01085.x>.
- [65] J.T. Paula, I.M.O. Sousa, M.A. Foglio, F.A. Cabral, Solubility of protocatechuic acid, sinapic acid and chrysin in supercritical carbon dioxide, *J. Supercrit. Fluids* 112 (2016) 89–94, <https://doi.org/10.1016/j.supflu.2016.02.014>.
- [66] W.L. Peng, H. Mohd-Nasir, S.H.M. Setapar, A. Ahmad, D. Lokhat, Optimization of process variables using response surface methodology for tocopherol extraction from Roselle seed oil by supercritical carbon dioxide, *Ind. Crops Prod.* 143 (2020) 111886, <https://doi.org/10.1016/j.indcrop.2019.111886>.
- [67] N.R. Putra, M.A.C. Yunus, S. Machmudah, Solubility model of arachis hypogea skin oil by modified supercritical carbon dioxide, *Sep. Sci. Technol.* 54 (5) (2019) 731–740, <https://doi.org/10.1080/01496395.2018.1520725>.
- [68] N. Recharla, M. Riaz, S. Ko, S. Park, Novel technologies to enhance solubility of food-derived bioactive compounds: a review, *J. Funct. Foods* 39 (2017) 63–73, <https://doi.org/10.1016/j.jff.2017.10.001>.
- [69] T.A. Reddy, C. Garlapati, Dimensionless empirical model to correlate pharmaceutical compound solubility in supercritical carbon dioxide, *Chem. Eng. Technol.* 42 (12) (2019) 2621–2630, <https://doi.org/10.1002/ceat.201900283>.
- [70] A. Rojas-Ávila, A. Pimentel-Rodas, T. Rosales-García, G. Dávila-Ortiz, L. A. Galicia-Luna, Solubility of binary and ternary systems containing vanillin and vanillic acid in supercritical carbon dioxide, *J. Chem. Eng. Data* 61 (9) (2016) 3225–3232, <https://doi.org/10.1021/acs.jced.6b00322>.
- [71] M.A. Sabegh, H. Rajaei, F. Esmailzadeh, M. Lashkarbolooki, Solubility of ketoprofen in supercritical carbon dioxide, *J. Supercrit. Fluids* 72 (2012) 191–197, <https://doi.org/10.1016/j.supflu.2012.08.008>.
- [72] M. Sahihi, H.S. Ghaziaskar, M. Hajebrahimi, Solubility of maleic acid in supercritical carbon dioxide, *J. Chem. Eng. Data* 55 (7) (2010) 2596–2599, <https://doi.org/10.1021/je9008393>.
- [73] S.A. Sajadian, M. Amani, N.S. Ardestani, S. Shirazian, Experimental analysis and thermodynamic modelling of lenalidomide solubility in supercritical carbon dioxide, *Arab. J. Chem.* 15 (6) (2022) 103821, <https://doi.org/10.1016/j.arabj.2022.103821>.
- [74] S.A. Sajadian, N.S. Ardestani, A. Jouyban, Solubility of montelukast (as a potential treatment of COVID -19) in supercritical carbon dioxide: experimental data and modelling, *J. Mol. Liq.* 349 (2022) 118219, <https://doi.org/10.1016/j.molliq.2021.118219>.
- [75] M. Shamsipur, A.R. Karami, Y. Yamini, H. Sharghi, A.R. Salimi, Solubilities of some thioxanthone derivatives in supercritical CO₂, *J. Chem. Eng. Data* 48 (5) (2003) 1088–1091, <https://doi.org/10.1021/je020163y>.
- [76] S.A. Shojaei, A.Z. Hezave, S. Aftab, M. Lashkarbolooki, F. Esmailzadeh, Solubility of gabapentin in supercritical carbon dioxide, *J. Supercrit. Fluids* 78 (2013) 1–6, <https://doi.org/10.1016/j.supflu.2013.02.003>.
- [77] C. Si-Moussa, A. Belghait, L. Khaouane, S. Hanini, A. Halilali, Novel density-based model for the correlation of solid drugs solubility in supercritical carbon dioxide, *Comptes Rendus Chimie* 20 (5) (2017) 559–572, <https://doi.org/10.1016/j.crci.2016.09.009>.
- [78] B.M.C. Soares, F.M.C. Gamarra, L.C. Pavianni, L.A.G. Gonçalves, F.A. Cabral, Solubility of triacylglycerols in supercritical carbon dioxide, *J. Supercrit. Fluids* 43 (1) (2007) 25–31, <https://doi.org/10.1016/j.supflu.2007.03.013>.
- [79] G. Sodeifan, R. Surya Alwi, F. Razmimanesh, Solubility of Pholcodine (antitussive drug) in supercritical carbon dioxide: experimental data and thermodynamic modeling, *Fluid Phase Equilib.* 556 (2022) 113396, <https://doi.org/10.1016/j.fluid.2022.113396>.
- [80] G. Sodeifan, M.A. Nooshabadi, F. Razmimanesh, A. Tabibzadeh, Solubility of buprenorphine hydrochloride in supercritical carbon dioxide: study on experimental measuring and thermodynamic modeling, *Arab. J. Chem.* 16 (10) (2023) 105196, <https://doi.org/10.1016/j.arabj.2023.105196>.
- [81] G. Sodeifan, M.M.B. Usefi, F. Razmimanesh, A. Roshanghias, Determination of the solubility of rivaroxaban (anticoagulant drug, for the treatment and prevention of blood clotting) in supercritical carbon dioxide: experimental data and correlations, *Arab. J. Chem.* 16 (1) (2023) 104421, <https://doi.org/10.1016/j.arabj.2022.104421>.
- [82] G. Sodeifan, R. Detakhsheshpour, S.A. Sajadian, Experimental study and thermodynamic modeling of Esomeprazole (proton-pump inhibitor drug for stomach acid reduction) solubility in supercritical carbon dioxide, *J. Supercrit. Fluids* 154 (2019) 104606, <https://doi.org/10.1016/j.supflu.2019.104606>.
- [83] G. Sodeifan, C. Garlapati, F. Razmimanesh, F. Sodeifan, Solubility of Amlodipine Besylate (Calcium Channel Blocker Drug) in supercritical carbon dioxide: measurement and correlations, *J. Chem. Eng. Data* 66 (2) (2021) 1119–1131, <https://doi.org/10.1021/acs.jced.0c00913>.
- [84] G. Sodeifan, S. Mojtaba Hazaveie, S. Ali Sajadian, N.S. Ardestani, Determination of the solubility of the repaglinide drug in supercritical carbon dioxide: experimental data and thermodynamic modeling, *J. Chem. Eng. Data* 64 (12) (2019) 5338–5348, <https://doi.org/10.1021/acs.jced.9b00550>.
- [85] G. Sodeifan, F. Razmimanesh, N. Saadati Ardestani, S.A. Sajadian, Experimental data and thermodynamic modeling of solubility of Azathioprine, as an immunosuppressive and anti-cancer drug, in supercritical carbon dioxide, *J. Mol. Liq.* 299 (2020) 112179, <https://doi.org/10.1016/j.molliq.2019.112179>.
- [86] G. Sodeifan, F. Razmimanesh, S.A. Sajadian, Prediction of solubility of sunitinib malate (an anti-cancer drug) in supercritical carbon dioxide (SC-CO₂): experimental correlations and thermodynamic modeling, *J. Mol. Liq.* 297 (2020) 111740, <https://doi.org/10.1016/j.molliq.2019.111740>.
- [87] G. Sodeifan, F. Razmimanesh, S.A. Sajadian, Solubility measurement of a chemotherapeutic agent (Imatinib mesylate) in supercritical carbon dioxide: assessment of new empirical model, *J. Supercrit. Fluids* 146 (2019) 89–99, <https://doi.org/10.1016/j.supflu.2019.01.006>.
- [88] G. Sodeifan, F. Razmimanesh, S.A. Sajadian, S.M. Hazaveie, Experimental data and thermodynamic modeling of solubility of Sorafenib tosylate, as an anti-cancer drug, in supercritical carbon dioxide: evaluation of Wong-Sandler mixing rule, *J. Chem. Thermodyn.* 142 (2020) 105998, <https://doi.org/10.1016/j.jct.2019.105998>.
- [89] G. Sodeifan, F. Razmimanesh, S.A. Sajadian, H.S. Panah, Solubility measurement of an antihistamine drug (Loratadine) in supercritical carbon dioxide: assessment of qCPA and PCP-SAFT equations of state, *Fluid Phase Equilib.* 472 (2018) 147–159, <https://doi.org/10.1016/j.fluid.2018.05.018>.
- [90] G. Sodeifan, N. Saadati Ardestani, S.A. Sajadian, M.R. Golmohammadi, A. Fazlali, Prediction of solubility of sodium valproate in supercritical carbon dioxide: experimental study and thermodynamic modeling, *J. Chem. Eng. Data* (2020), <https://doi.org/10.1021/acs.jced.9b01069>.
- [91] G. Sodeifan, N. Saadati Ardestani, S.A. Sajadian, M.R. Golmohammadi, A. Fazlali, Prediction of solubility of sodium valproate in supercritical carbon dioxide: experimental study and thermodynamic modeling, *J. Chem. Eng. Data* 65 (4) (2020) 1747–1760, <https://doi.org/10.1021/acs.jced.9b01069>.
- [92] G. Sodeifan, S.A. Sajadian, Experimental measurement of solubilities of sertraline hydrochloride in supercritical carbon dioxide with/without menthol: data correlation, *J. Supercrit. Fluids* 149 (2019) 79–87, <https://doi.org/10.1016/j.supflu.2019.03.020>.
- [93] G. Sodeifan, S. Ali Sajadian, N.S. Ardestani, Determination of solubility of Aprepitant (an antiemetic drug for chemotherapy) in supercritical carbon dioxide: empirical and thermodynamic models, *J. Supercrit. Fluids* 128 (2017) 102–111, <https://doi.org/10.1016/j.supflu.2017.05.019>.
- [94] G. Sodeifan, S. Ali Sajadian, F. Razmimanesh, Solubility of an antiarrhythmic drug (amiodarone hydrochloride) in supercritical carbon dioxide: experimental and modeling, *Fluid Phase Equilib.* 450 (2017) 149–159, <https://doi.org/10.1016/j.fluid.2017.07.015>.
- [95] S. Soltani, S.H. Mazloumi, A new empirical model to correlate solute solubility in supercritical carbon dioxide in presence of co-solvent, *Chem. Eng. Res. Des.* 125 (2017) 79–87, <https://doi.org/10.1016/j.cherd.2017.07.006>.
- [96] D.L. Sparks, R. Hernandez, L.A. Estévez, Evaluation of density-based models for the solubility of solids in supercritical carbon dioxide and formulation of a new model, *Chem. Eng. Sci.* 63 (17) (2008) 4292–4301, <https://doi.org/10.1016/j.ces.2008.05.031>.
- [97] Y.Y. Sun, S.F. Li, Measurement and correlation of the solubility of Ligusticum Chuanxiong oil in supercritical CO₂, *Chin. J. Chem. Eng.* 13 (2005) 796–799.
- [98] K. Tomita, S. Machmudah, A. Quitain, M. Sasaki, R. Fukuzato, M. Goto, Extraction and solubility evaluation of functional seed oil in supercritical carbon dioxide, *J. Supercrit. Fluids* 79 (2013) 109–113, <https://doi.org/10.1016/j.supflu.2013.02.011>.
- [99] C.-C. Tsai, H.-M. Lin, M.-J. Lee, Solubility of niflumic acid and celecoxib in supercritical carbon dioxide, *J. Supercrit. Fluids* 95 (2014) 17–23, <https://doi.org/10.1016/j.supflu.2014.07.026>.
- [100] M.-C. Wei, J. Xiao, Y.-C. Yang, Extraction of α -humulene-enriched oil from clove using ultrasound-assisted supercritical carbon dioxide extraction and studies of its fictitious solubility, *Food Chem.* 210 (2016) 172–181, <https://doi.org/10.1016/j.foodchem.2016.04.076>.
- [101] Y. Yamini, J. Hassan, S. Haghgo, Solubilities of some nitrogen-containing drugs in supercritical carbon dioxide, *J. Chem. Eng. Data* 46 (2) (2001) 451–455, <https://doi.org/10.1021/je000286n>.
- [102] Y. Yamini, M. Tayyebi, M. Moradi, A. Vatanara, Solubility of megestrol acetate and levonorgestrel in supercritical carbon dioxide, *Thermochim. Acta* 569 (2013) 48–54, <https://doi.org/10.1016/j.tca.2013.07.018>.

- [103] F. Zabihi, M. Mirzajanzadeh, J. Jia, Y. Zhao, Measurement and calculation of solubility of quinine in supercritical carbon dioxide, *Chin. J. Chem. Eng.* 25 (5) (2017) 641–645, <https://doi.org/10.1016/j.cjche.2016.10.003>.
- [104] A. Zeinolabedini Hezave, F. Esmailzadeh, Solubility measurement of diclofenac acid in the supercritical CO₂, *J. Chem. Eng. Data* 57 (6) (2012) 1659–1664, <https://doi.org/10.1021/je200012x>.
- [105] S. Zhan, S. Li, Q. Zhao, W. Wang, J. Wang, Measurement and correlation of curcumin solubility in supercritical carbon dioxide, *J. Chem. Eng. Data* 62 (4) (2017) 1257–1263, <https://doi.org/10.1021/acs.jced.6b00798>.
- [106] S. Zhan, H. Miao, Yu Zhao, J. Wang, Z. Li, Experimental determination and association model for the solubility of Laminarin in supercritical carbon dioxide, *J. Chem. Eng. Data* 65 (4) (2020) 1814–1823, <https://doi.org/10.1021/acs.jced.9b01084>.
- [107] S. Zhao, D. Zhang, An experimental investigation into the solubility of Moringa oleifera oil in supercritical carbon dioxide, *J. Food Eng.* 138 (2014) 1–10, <https://doi.org/10.1016/j.jfoodeng.2014.03.031>.
- [108] M.H. Zuknik, N.A. Nik Norulaini, W.S. Wan Nursyazreen Dalila, N.R. Ali, A. K. Mohd Omar, Solubility of virgin coconut oil in supercritical carbon dioxide, *J. Food Eng.* 168 (2016) 240–244, <https://doi.org/10.1016/j.jfoodeng.2015.08.004>.